



HAL
open science

Toward a computational and experimental model of a poly-epoxy surface

Thomas Duguet, Camille Bessaguet, Maëlen Aufray, Jérôme Esvan, Cédric Charvillat, Constantin Vahlas, Corinne Lacaze-Dufaure

► **To cite this version:**

Thomas Duguet, Camille Bessaguet, Maëlen Aufray, Jérôme Esvan, Cédric Charvillat, et al.. Toward a computational and experimental model of a poly-epoxy surface. *Applied Surface Science*, 2015, vol. 324, pp. 605-611. 10.1016/j.apsusc.2014.10.096 . hal-01105225

HAL Id: hal-01105225

<https://hal.science/hal-01105225>

Submitted on 20 Jan 2015

HAL is a multi-disciplinary open access archive for the deposit and dissemination of scientific research documents, whether they are published or not. The documents may come from teaching and research institutions in France or abroad, or from public or private research centers.

L'archive ouverte pluridisciplinaire **HAL**, est destinée au dépôt et à la diffusion de documents scientifiques de niveau recherche, publiés ou non, émanant des établissements d'enseignement et de recherche français ou étrangers, des laboratoires publics ou privés.



Open Archive Toulouse Archive Ouverte (OATAO)

OATAO is an open access repository that collects the work of Toulouse researchers and makes it freely available over the web where possible.

This is an author-deposited version published in: <http://oatao.univ-toulouse.fr/>
Eprints ID: 12279

Identification number: DOI : 10.1016/j.apsusc.2014.10.096
Official URL: <http://dx.doi.org/10.1016/j.apsusc.2014.10.096>

To cite this version:

Duguet, Thomas and Bessaguet, Camille and Aufray, Maëlen and Esvan, Jérôme and Charvillat, Cédric and Vahlas, Constantin and Lacaze-Dufaure, Corinne *Toward a computational and experimental model of a poly-epoxy surface*. (2015) Applied Surface Science, vol. 324 . pp. 605-611. ISSN 01694332

Any correspondence concerning this service should be sent to the repository administrator:
staff-oatao@inp-toulouse.fr

Toward a computational and experimental model of a poly-epoxy surface

Thomas Duguet*, Camille Bessaguet, Maëleonn Aufray, Jérôme Esvan, Cédric Charvillat, Constantin Vahlas, Corinne Lacaze-Dufaure

CIRIMAT, CNRS – Université de Toulouse, 4, allée Emile Monso, BP-44362, 31030 Toulouse Cedex 4, France

A B S T R A C T

A model poly-epoxy surface formed by the reaction of DGEBA and EDA is studied by the combination of experiments and DFT calculations. A special synthesis protocol is presented leading to the formation of a surface that is smooth ($S_a < 1$ nm), chemically homogeneous, and that presents a low-defect density ($0.21 \mu\text{m}^{-2}$), as shown by AFM characterizations. Then, XPS is used for the determination of the elemental and functional groups' surface composition. DFT allows the identification and assignment of individual bonds contributions to the experimental 1s core-level peaks. Overall, we demonstrate that such a model sample is perfectly suitable for a use as a template for the study of poly-epoxy surface functionalization.

Keywords:

Epoxy
Amine
Surface science
AFM
XPS
DFT

1. Introduction

Poly-epoxy polymers are widely implemented in three families of applications: adhesives, paints, and composite materials [1]. The latter, such as epoxy/C fibers composites are increasingly found in a wealth of devices and parts in the fields of leisure (skis, rackets, boats, golf clubs, etc.), or transports, aeronautics and space (cars, aircrafts, satellites, etc.), to name but a few. These composite materials possess stiffness and Young's modulus that compare well with metallic alloys but with a much lower chemical reactivity and density. Therefore, they allow mass reduction and a large increase of parts durability.

Replacement of metallic or ceramic parts by polymers often requires surface functionalization in order to acquire optical, electrical, magnetic, biomedical, esthetic, or chemical properties. The main drawback when it comes to coat or to graft the surface of polymer-based composites comes from the very low surface energy of such materials once polymerized. This leads to a poor wettability rendering painting or gluing difficult, and resulting in poor adhesion. The surface energy of poly-ether ether ketone (PEEK) or poly-epoxy is approximately $40\text{--}50 \text{ mJ/m}^2$ to be compared to

approximately 500 mJ/m^2 for aluminum. Moreover, the polar component (due to H bonding) is as low as $6\text{--}7 \text{ mJ/m}^2$ which inhibits the use of simple functionalization protocols [2–4]. Hence, a large number of particular protocols has been described or patented, where the increase of reactivity and roughness is sought. A selection amongst the wealth of publications can be found in Refs. [5–16].

Such protocols or methods that have been used until now remain empirical despite the resulting improvement of the targeted properties and/or the extension of the durability of the material. Therefore, the need exists to access the basic mechanisms which control the surface functionalization of polymers and to control them so as to achieve satisfactory functional properties and adhesion. By subscribing in this perspective, our approach aims at describing the nucleation and growth of metallic thin films on polymer surfaces, by using an integrated method where all the elementary mechanisms are taken into account. The first step in this frame – object of the present study – is to obtain a model of the polymer surface, both experimental and theoretical, at the atomic/molecular level. Such a model will serve as a template for further surface treatments, including pretreatments, molecular grafting, or application of films and coatings. It is worth noting that, to the authors' knowledge, no such a theoretical surface model exists, most likely because of structural disorder and a lack of experimental inputs.

* Corresponding author. Tel.: +33 05 34 32 34 39.
E-mail address: thomas.duguet@ensiacet.fr (T. Duguet).

Regarding our objectives, specifications of such an experimental model polymer surface include:

- A 100% polymerization after curing to be comparable with calculations, where total polymerization is assumed.
- A low surface arithmetic roughness, namely $R_a < 1$ nm to make sure that we can observe nano-islands or nano-clusters of a given thin film. Otherwise, they would be hindered by roughness.
- A very low defect density to avoid heterogeneous nucleation at defects.
- Chemical homogeneity to make sure that calculation models where homogeneity is assumed are representative of the tracked chemical reactivity. Also to make sure that chemical composition is independent on the analyzed surface area corresponding to a given probe size.

Our experimental approach is based on the method described in [17,18] for forming model poly-epoxy surfaces. It consists in the polymerization of the poly-epoxy in an Ar gloves box at ambient temperature for at least 24h, followed by a post-curing at elevated temperature (polymer-dependent). Gu et al. [17] synthesize samples from a stoichiometric mixture of DGEBA + 1,3-di(aminomethyl)-cyclohexane, with a small amount of toluene for decreasing viscosity and favoring an homogeneous stirring (7 min). Samples are then stored for 24 h at ambient temperature, and post-cured for 2 h at 130 °C in an air furnace. Characterizations of the free surfaces are performed by atomic force microscopy (AFM) in Tapping[®] mode. Surface roughness and phase contrast are determined. It is shown that samples synthesized in an Ar glove box show a lower surface roughness than those prepared in ambient conditions, and that they are homogeneous in composition. Kansow et al. [18] use a similar method with the aim of characterizing the formation of Al, Cu, Ag, and Au films by physical vapour deposition. DGEBA reacts with diethylene triamine in low excess at 55 °C under controlled atmosphere, before it is left for 48 h at ambient temperature. At this step, polymerization rate is about 75%. Completion is achieved by post curing for 1 h at 120 °C. Surface roughness is about 1 nm.

Theoretically, our greatest challenge is to circumvent the description of the disordered/amorphous structure and to limit the number of atoms. To that end, we start with a small macromolecule made from the reaction of bisphenol A diglycidyl ether (DGEBA) with ethylenediamine (EDA) (61 atoms). Even for this moderately complex system, the analysis of the experimental core-level XPS spectrum is not trivial and can lead to incorrect conclusions. The help of accurate theoretical tools is thus needed and density-functional theory (DFT) is usually used for computing XPS core-level shifts in the case of small organic or inorganic systems. The application of this theoretical method to large systems, e.g. polymers, is a challenge but it is established that experimental spectra are directly related to the electronic states obtained from calculations on smaller model molecules. For instance, Endo et al. presented a comprehensive analysis of the XPS C 1s spectra for polymers using the negative of the energy of molecular orbitals [19,20]. More recently, they used the 'transition state' theory [21] for the calculation of the core electron binding energies [22,23]. Following this work and in a first approach, we compute the molecular orbitals energies on model molecules as preliminary input for the assignment of experimental XPS spectra of the investigated polymer.

We complement these results in the different DGEBA + EDA system by implementing a more detailed description of surfaces by AFM and XPS characterizations complemented by DFT calculations. The paper is organized as follows. Experimental and computational

details are given in Section 2, followed by results in Section 3. Conclusions and perspectives are presented in Section 4.

2. Experimental and computational details

2.1. Synthesis

We use a stoichiometric mixture of DGEBA (DER 332, Dow Chemicals, $n=0.03$) and EDA (analytical grade, purity >99.5%, Sigma Aldrich). The mass of DGEBA (m_{DGEBA}) is fixed to 5 g. The mass of EDA m_{EDA} is thus determined following Eq. (1).

$$m_{DAE} = \frac{f_{DGEBA}}{f_{DAE}} \times \frac{M_{DAE} \times m_{DGEBA}}{M_{DGEBA}} = 0.43 \text{ g} \quad (1)$$

where M_{DGEBA} is the molar mass (348.52 g/mol) of this DGEBA and f_{DGEBA} is its functionality (2), and M_{EDA} is the molar mass (60.10 g/mol) and f_{DAE} is the functionality (4) of the EDA. We assume that no etherification occurs.

The mixture is then mechanically stirred (in an Ar glove box when specified) for 7 min before it is poured into different molds or deposited as a thin droplet on aluminum foil. Polymerization is then allowed for 48 h at ambient temperature, followed by a post curing of 2 h at 140 °C. For roughness comparison, we consider the following poly-epoxy surfaces formed:

- At free surfaces, surfaces ref. either epoxy^{Air} or epoxy^{Argon}.
- At the interface with a 1 cm × 1 cm × 0.2 cm silicone mold, itself molded on a Si wafer for transferring atomic flatness. Interfaces ref. SiO_{Si}/epoxy^{Air} or SiO_{Si}/epoxy^{Argon}.
- At the interface with a 1 cm × 1 cm × 0.2 cm silicone mold, itself molded on polystyrene (PS). Interfaces ref. SiO_{PS}/epoxy^{Air} or SiO_{PS}/epoxy^{Argon}.
- By mechanical polishing up to a ¼ μm with diamond paste. Surfaces ref. polished^{Air}.

Interfaces formed in the same molds but in air or Ar show different roughnesses (shown hereafter). This is the reason why SiO_{Si}/epoxy^{Air} and SiO_{Si}/epoxy^{Argon}, and SiO_{PS}/epoxy^{Air} and SiO_{PS}/epoxy^{Argon} are differentiated.

2.2. Bulk characterizations

Differential scanning calorimetry (DSC) is used for the determination of the glass transition temperature (T_g) of the poly-epoxy under investigation. We use a DSC 204 Phoenix Series (NETZSCH) coupled with a TASC 414/4 controller. The apparatus is calibrated against melting temperatures of In, Hg, Sn, Bi, and Zn, applying a +10°/min temperature ramp. Samples are placed in aluminum capsules. Mass is measured with an accuracy of ±0.1 mg. We choose to report the onset $T_{g\text{-onset}}$ temperature.

Fourier transform infrared spectroscopy, FTIR (Frontier, PerkinElmer equipped with a NIR TGS detector), is performed in transmission in the 4000–8000 cm⁻¹ range. 16 scans are collected for each analysis with a resolution of 4 cm⁻¹. We monitor the characteristic epoxy band (combination band of the -CH₂ of the epoxy group) at 4530 cm⁻¹ with increasing polymerization time, and after post curing treatment. The reference band is the combination band of C=C with aromatic -CH at 4623 cm⁻¹ [24]. Peak areas are then used for calculating the conversion rate (X_{eNIR}) of epoxy groups, following Eq. (2).

$$X_{eNIR} = 1 - \frac{(A_{epoxy}/A_{reference})_{t=t}}{(A_{epoxy}/A_{reference})_{t=0}} \quad (2)$$

where A_{epoxy} and $A_{reference}$ are the peak areas of the epoxy and reference groups, respectively.

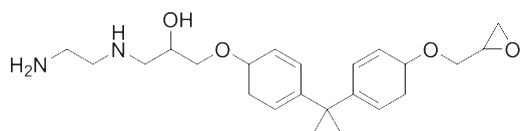


Fig. 1. Model dimer (1 DGEBA + 1 EDA).

2.3. Surface characterizations

Surface roughness and viscoelastic homogeneity are determined by AFM (Agilent Technologies model 5500) in ambient conditions. The former is performed in contact mode with tips of spring constant k approx. 0.292 N/m , whereas the latter is performed in Tapping[®] mode with tips of $k = 25\text{--}75\text{ N/m}$ (AppNano). Scanning rate is $2\ \mu\text{m/s}$. Images are processed with the softwares Gwyddion version 2.19 [25] and Pico Image (Agilent Technologies). Surface roughness parameters follow the Geometric Product Specifications ISO 25178. S_a is the arithmetic roughness, S_q is the root mean square roughness, and S_z is the total roughness (maximum peak-to-valley), determined by processing the AFM images.

XPS analysis is performed using a Thermoelectron Kalpha apparatus. Photoemission spectra are recorded using Al-K α radiation ($h\nu = 1486.6\text{ eV}$) from a monochromatized source. The X-ray spot diameter on the sample surface is $400\ \mu\text{m}$. The pass energy is fixed at 30 eV for narrow scan and 170 eV for survey scans. The spectrometer energy calibration was performed using the Au $4f^{7/2}$ ($83.9 \pm 0.1\text{ eV}$) and Cu $2p^{3/2}$ ($932.8 \pm 0.1\text{ eV}$) photoelectron lines. The background signal is removed using the Shirley method. Atomic concentrations are determined from photoelectron peak areas using the atomic sensitivity factors reported by Scofield [26] and taking into account the transmission function of the analyzer. This function was determined at different pass energies from Ag 3d and Ag MNN peaks collected on a silver standard. Finally, photoelectron peaks are analyzed and deconvoluted using a Lorentzian/Gaussian ($L/G = 30$) peak fitting.

2.4. Calculations

We used the model molecule shown in Fig. 1 that results of the addition of one DGEBA and one EDA molecule.

The geometry of the model molecule was optimized at the B3LYP/6-31G* level of theory using the Gaussian 03 software package [27].

3. Results

Bulk characterizations are performed on samples polymerized under ambient conditions. DSC is used for the determination of $T_{g\text{-onset}}$. Temperature ramps are doubled for each sample in order to ensure that there is no physical aging and to verify that polymerization is complete. For all samples $T_{g\text{-onset}} = 113 \pm 1\text{ }^\circ\text{C}$. We assume that $T_{g\text{-onset}}$ is not different after polymerization in the Ar glove box (no bulk characterization for these samples).

We then monitor the polymerization rate with reaction duration by following the gradual decrease of the epoxy peak area by FTIR, and calculating the conversion rate using Eq. (2). Results are shown in Fig. 2.

Experiments are performed from 15 min to 11520 min (8 days) after mixing of the reactants. The conversion rate increases slowly in the first hours and reaches an asymptote between 24 and 48 h. The maximum conversion at ambient temperature is 84% for $t \geq 48\text{ h}$. The only mean for achieving a complete polymerization is to set the sample at a temperature above its glass transition. The post curing treatment ($140\text{ }^\circ\text{C}$, 2 h) leads to a complete

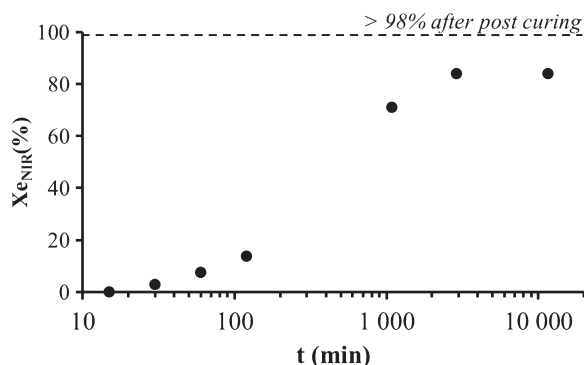


Fig. 2. Epoxy group conversion rate as a function of polymerization over an 8-day period of time. Dashed line indicates that polymerization is complete after post curing at $140\text{ }^\circ\text{C}$ for 2 h.

polymerization ($>98\%$, taking into account the FTIR spectrometer sensitivity) illustrated by the dashed line in Fig. 2.

The different surfaces that we consider are then characterized by AFM over $3\ \mu\text{m} \times 3\ \mu\text{m}$ surface area images in order to determine roughness parameters. Results are summarized in Fig. 3.

Roughness of the free surfaces is reduced by three orders of magnitude when polymerization is performed in the Ar glove box. Under Ar, S_a and S_q do not exceed 1.5 nm , except for sample $\text{SiO}_{\text{Si}}/\text{epoxy}^{\text{Argon}}$, for which these two values are 4.9 nm and 6.8 nm , respectively. The latter is not acceptable for the AFM observation of metallic nanoislands or clusters that we target, in the range of $1\text{--}20\text{ nm}$ in diameter [18]. In order to transfer atomic flatness to the molds, and then to the $\text{SiO}_{\text{Si}}/\text{epoxy}$ surfaces, we mold silicone molds against Si wafer or against PS. In these conditions, the lowest roughness is again obtained when the surfaces are formed under Ar atmosphere, and is similar between Si and PS processes. Somehow, atmosphere also plays a role regarding roughness at the substrate/polymer interface. However, a roughness as low as at that of the free epoxy^{Argon} surface is not achieved, indicating that molding in these conditions is not well suited for our purpose. Finally, the roughness parameters of the polished surface are quite low but AFM images show many scratches where nucleation may preferentially occur. Since we want to avoid heterogeneous nucleation in order to compare nucleation with adsorption energies at the molecular level, polishing is abandoned.

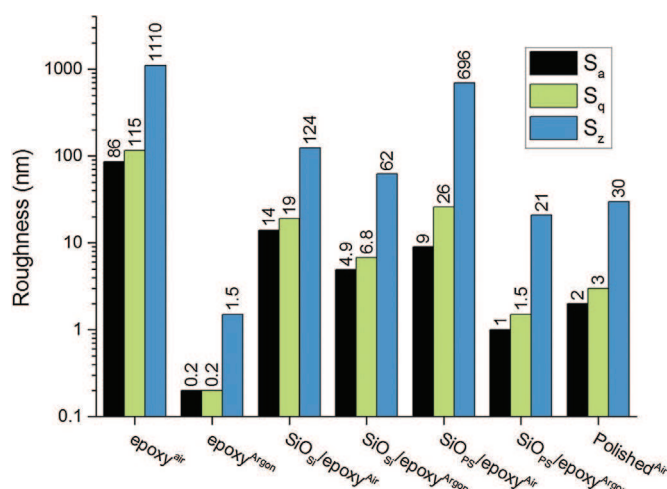


Fig. 3. Roughness parameters determined by image processing on $3\ \mu\text{m} \times 3\ \mu\text{m}$ surfaces characterized by AFM in contact mode. A polynomial of degree 2 is used in order to correct image curvature.

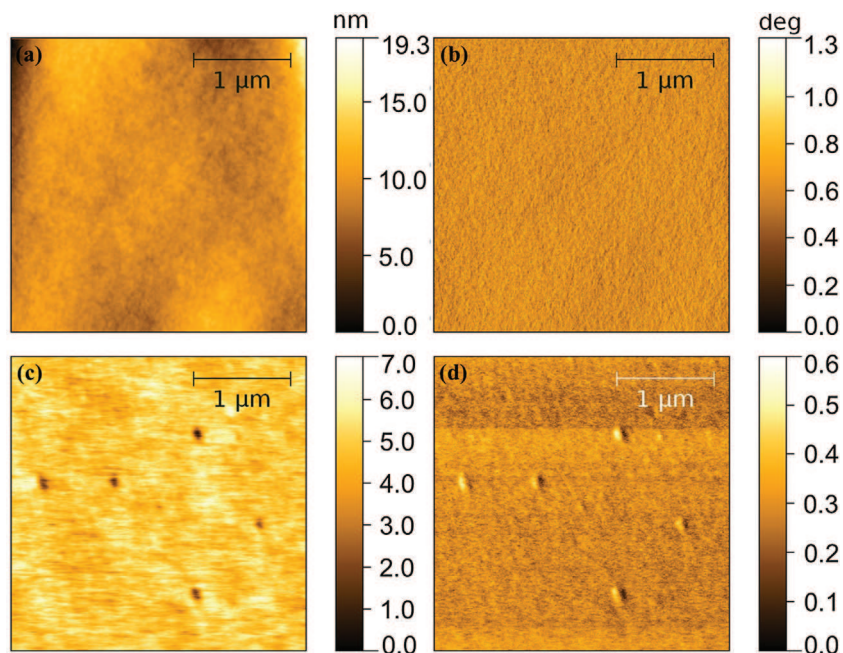


Fig. 4. AFM images of the epoxy^{Air} (a and b) and epoxy^{Argon} (c and d) surfaces. Left column shows topographic images after a polynomial of degree 2 correction, and right column shows deflection images (or phase contrast).

Fig. 4 shows a selection of AFM images of the epoxy^{Air} (a and b) and epoxy^{Argon} (c and d) surfaces, obtained in Tapping[®] mode. Right column (Fig. 4a and c) corresponds to the surface topography and left column (Fig. 4b and d) to the deflection of the cantilever, i.e. to the phase contrast. Whereas Tapping[®] mode leads to different apparent values of roughness compared to contact mode, roughness is again lower on the epoxy^{Argon} surface, as can be noticed on the contrast scale, on the right-hand side of the images. However, both surfaces are quite flat and exhibit a very low phase contrast. The measure of phase contrast probes the local viscoelastic properties that we assume to be an indication of chemical homogeneity in the nanometer range. Finally, Fig. 4c and d is chosen on purpose in order to illustrate the presence of defects, in the form of approx. 50 nm-in-diameter troughs. The density shown in Fig. 4 is not representative (overestimated). A thorough count over a total 90 μm² surface area gives a defect density equal to 0.21 μm⁻².

Epoxy^{Argon} is selected as the best candidate for an experimental model surface of poly-epoxy. Thus, we investigate its surface chemical composition by XPS and use the output of DFT calculations for peak identifications and binding energy assignments. A first observation is made on free surfaces of samples synthesized in silicone molds (i.e. that were not in contact with the mold). Survey spectra show a strong Si 2p contribution at 101.8 ± 0.1 eV, which is characteristic of siloxane groups [28]. It represents a large amount of adsorbed silicone on the surface (approx. 8 at.%). Consequently, epoxy^{Air} samples are now synthesized on Al foil (and silicone is banished from the glove box). The significant thickness of the poly-epoxy coupons (1 mm) ensures that Al does not diffuse up to the free surface, since the measured interphases do not exceed 300 μm [29].

The XPS survey spectrum of epoxy^{Argon} surfaces polymerized on aluminum foil show neither Si nor other elements than the one expected in the polymer or from adsorbed molecules from the air. Atomic composition of the surface is determined by 1s peaks fitting, repeated at different x - y coordinates on the sample surface. We determine the following surface composition:

81.5 at.%C, 1.8 at.%N, and 16.7 at.%O

The result is slightly different from the bulk composition of the poly-epoxy, where the basic motif is made of 2 DGEBA (2×21 C + 2×4 O atoms) molecules for 1 EDA (2 C + 2 N atoms) molecule, resulting in a bulk composition of: 81.5 at. % C, 3.7 at. % N, and 14.8 at. % O. Whereas the composition of the surface shows a similar carbon content, it is richer in oxygen and poorer in nitrogen than the bulk. This is an indication of a mild surface oxidation that may occur in the course of post-curing, when polymerization is not yet complete (post-curing starts at 85% polymerization rate). It is questioning though that the carbon content is apparently not affected as well.

In order to further investigate the surface chemistry of the model poly-epoxy surface, molecular orbitals extracted directly from DFT results are studied. Table 1 shows the binding energies of 1s electrons involved in the different bonds of the model dimer. The dimer is made of 1 DGEBA and 1 EDA that virtually bonded through 1 epoxy/1 amine proton reaction. Therefore, there are a few discrepancies between the experimental fully-polymerized samples and the model dimer. They are enlightened by the gray coloring of the lines corresponding to secondary and primary amines (all should be ternary) and to the epoxy group (no more epoxy rings in the 100% polymerized sample). The binding energies shown are the negative value of the molecular orbitals energies. Therefore, absolute values are not correct because (i) XPS binding energies correspond to a multi-step process where photoelectrons interact with the created holes, with the matrix and with their image before and after extraction into vacuum, (ii) temperature is not considered, (iii) of the limitation of Kohn-Sham orbital energies as reflecting initial state effects [30]. Nevertheless, chemical shifts can be used if one consider the latter processes constant in a given energy domain.

A minimum mean chemical shift of 0.2 eV is technically observable with our XPS apparatus. Therefore, we discriminate phenyl groups from $-\text{CH}_3$ groups, and C-OH & part of the C-O-C bonds from the other C-O-C bonds. Thanks to the support of DFT results, we use 5 contributions to the C 1s peak deconvolution and 2 contributions to the O 1s peak deconvolution. The fine fitting of the C 1s and O 1s spectra are shown in Fig. 5. N 1s spectrum is not shown because it exhibits only one contribution for C-N bonds centered

Table 1

Molecular orbitals involving O, N, and C 1s atomic orbitals from DFT calculations on the model DGEBA-EDA dimer. Corresponding electronic binding energies ($(-1) \times$ orbital energy), and mean chemical shifts for the given bond. Grayed cells do not have a counterpart in the experimental fully-reticulated poly-epoxy.

Molecular orbital	Binding energy (Hartree)	Binding energy (eV)	Mean chemical shift (± 0.1 eV)	Bond
O 1s	-19.177	521.8	+0.8	C—O—C
	-19.170	521.6		C—O—C
	-19.165	521.5	+0.6	Epoxy
	-19.145	520.9	Ref.	O—H
N 1s	-14.324	389.8	+0.3	Secondary amine
	-14.316	389.5	Ref.	Primary amine
C 1s	-10.249	278.9	+2.0	C—O—C
	-10.249	278.9		C—O—C
	-10.246	278.8		C—O—C
	-10.244	278.7		C—O—C
	-10.239	278.6	+1.8	C—O—C
	-10.239	278.6		C—O—C
	-10.238	278.6		C—OH
	-10.212	277.9	+1.0	C—N
	-10.209	277.8		C—N
	-10.207	277.7		C—N
	-10.205	277.7		Quaternary C—C
	-10.186	277.2	+0.2	Phenyl
	-10.185	277.1		Phenyl
	-10.185	277.1		Phenyl
	-10.183	277.1		Phenyl
	-10.182	277.1		Phenyl
	-10.181	277.0		Phenyl
	-10.181	277.0		Phenyl
	-10.181	277.0		Phenyl
	-10.180	277.0		Phenyl
-10.176	276.9		Phenyl	
-10.173	276.8	0.0	—CH ₃	
-10.173	276.8	Ref.	—CH ₃	

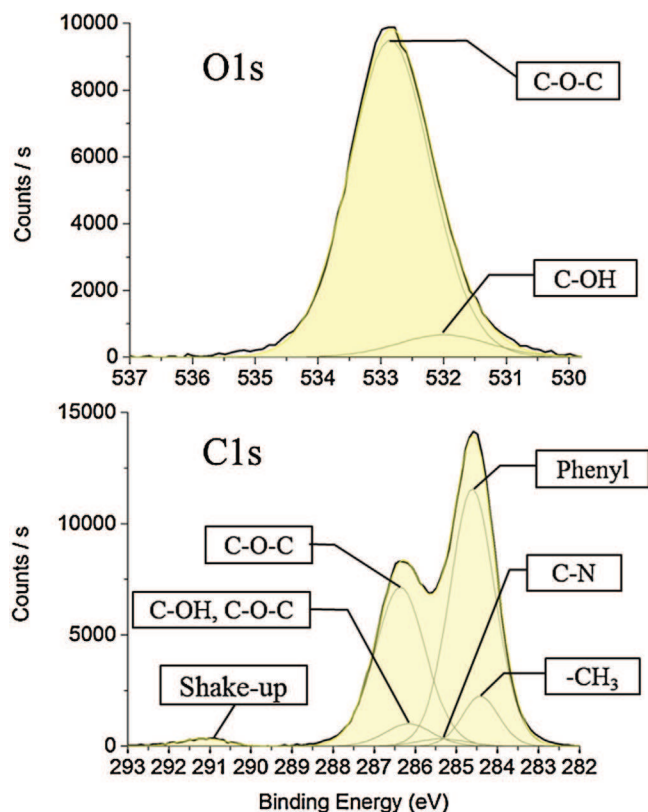


Fig. 5. XPS fine spectra of C 1s and O 1s. Spectra are fitted with contributions derived from DFT calculations on the model dimer.

at 399.2 eV. Binding energy scale of the C 1s spectrum starts with the —CH₃ contribution fixed at 284.4 eV. Then, mean chemical shifts extracted from the energy difference between molecular orbitals of DFT (see Table 1) are used for higher-binding-energy contributions (284.4 + 0.2, +1.0, +1.8, +2.0 eV).

The filled area shows the envelope of the fitting curve. There is an excellent matching with both O and C 1s experimental spectra. Again, calculations ensure that contributions are real; even C—N, for instance, which is buried in the tails of neighboring contributions. In order to consolidate these results, we now discuss fitting with regards to the functional group composition shown in Table 2.

Experimental atomic compositions in functional groups are consistent. For instance, where one O 1s orbital of the C—O—C bonds shows a composition of 15.5 at.%, two C 1s orbitals of the C—O—C bonds show an approximately doubled composition of 30.5 at.% (28.0 plus the contribution of C—O—C at 286.2 eV of about 3.7 (C 1s C—O—C, C—OH) - 1.2 (O 1s C—OH) = 2.5 at.%). Similarly, N 1s and C 1s compare well in terms of composition in the C—N bonds (1.8 vs. 1.3 at.%). Finally, the last column of Table 2 shows the expected composition in functional groups in a poly-epoxy where the DGEBA:EDA ratio equals 2:1. For instance the number of C 1s in phenyl groups is calculated as follows: 2 DGEBA \times 2 phenyls/DGEBA \times 6 C atoms = 24 C 1s. Overall, one can find 4 C 1s in —CH₃, 24 C 1s in phenyls, 2 C 1s in C—N, 4 C 1s in C—OH, 4 C 1s in C—O—C_{286.2 eV}, 4 C 1s in C—O—C_{286.4 eV}, 2 N 1s in C—N, 4 O 1s in C—OH, and 4 O 1s in C—O—C. Therefore the total number of considered 1s orbitals is 52. We observe large discrepancies concerning the phenyl bonds concentration and the oxygenated bonds C—OH and C—O—C concentrations, a difference that was already mentioned when considering the elemental atomic composition. There are two possibilities for explaining these differences: either the surface is oxidized and oxygenated bonds contribute to the C 1s and O 1s signals at neighboring binding energies, or the polymer is oriented in such a way that C—O—C bonds emerge at the surface.

Table 2

Results of the C, O, and N 1s deconvolutions; peak binding energy: BE, chemical shift imposed after DFT results; height in counts per second: CPS; full width at half-maximum: FWHM; peak area; scofield relative sensitivity factor: RSF; atomic fraction: at.%; and the composition expected from the model polymer with a DGEBA:EDA ratio of 2:1.

Name	Peak BE (eV)	Chemical shift (eV)	Height (CPS)	FWHM (eV)	Area (CPS eV)	Scofield RSF	At.%	2 DGEBA:EDA motif (at.%)
C 1s —CH ₃	284.4	0.0	2249.74	1.06	2578.62	1	6.5	7.7
C 1s phenyl	284.6	0.2	11580.87	1.3	16279.01	1	40.8	46.2
C 1s C—N	285.4	1.0	328.14	1.41	500.77	1	1.3	3.8
C 1s C—O—C, C—OH	286.2	1.8	1009.93	1.36	1488.52	1	3.7	C—OH:7.7 + C—O—C:7.7
C 1s C—O—C	286.4	2.0	7147.92	1.44	11172.06	1	28.0	7.7
C 1s shake up	291.2	n/a	349.91	1.32	501.28	1	1.3	n/a
N 1s C—N	399.2	n/a	808.92	1.28	1195.36	1.8	1.8	3.8
O 1s C—OH	532.0	0.0	669.53	1.73	1255.76	2.93	1.2	7.7
O 1s C—O—C	532.9	0.9	9494.3	1.53	15728.75	2.93	15.5	7.7

If we assume that a mild oxidation occurred in the course of sample preparation, it may be assigned to sub-stoichiometric groups, such as amines (1.3–1.8 vs. 3.8 at.% expected) and phenyls (40.8 vs. 46.2 at.% expected). In that case deconvolution may be improved by substituting or implementing additional contributions that we are not able to identify now.

4. Conclusions

We selected an epoxy-amine system which permits its use as both an experimental and a computational template for further surface treatments. DGEBA and EDA mixed in stoichiometric ratio and slowly polymerized (48 h) in an Ar glovebox lead to the formation of a poly-epoxy polymerized at a rate of 85%. Total polymerization is achieved by post-curing at 120 °C for 2 h. Such a poly-epoxy exhibits a glass transition temperature onset of 113 ± 1 °C. Different substrates and atmospheres were tested and compared in terms of surface roughness. The lowest roughness (arithmetic roughness = 0.2 nm, peak-to-valley = 1.5 nm) is obtained at the free surface that polymerized under Ar atmosphere. AFM observations reveal that, in addition to the high smoothness, the defect density of the surface is low enough to avoid defect driven undesirable nucleation. Additionally, phase contrast is almost null which indicates that the surface is chemically homogeneous. Atomic compositions from XPS survey spectra at different positions confirm this result. Fine XPS spectra over C, O, and N 1s core levels are analyzed in view of the DFT calculations results. Theoretical binding energy chemical shifts allow an excellent fitting of the experimental 1s spectra. A limitation has been emphasized concerning the compositions in chemical groups: the main discrepancy concerning a much larger composition in C—O—C than the one theoretically expected from the perfect polymer model. In a near future, we will dedicate our efforts to the improvement of (i) the poly-epoxy network model by allowing a larger number of atoms and by using molecular dynamics computations to freeze the structure at given temperatures, and (ii) of the core-level binding energies calculations using the generalized transition state method [21] that allows a better treatment of the XPS photoemission process. Finally, the perspectives for experimental work will be the formation of thin metallic films and the mechanistic description of nucleation and growth.

References

- [1] J.-P. Pascault, H. Sautereau, J. Verdu, R.J.J. Williams, *Thermosetting Polymers*, CRC Press, New York, 2002.
- [2] J.W. Gooch, *Encyclopedic Dictionary of Polymers*, Springer, New York, 2010.
- [3] E.M. Petrie, *Epoxy Adhesives Formulation*, McGraw-Hill, New York, 2006.
- [4] E.M. Petrie, *Handbook of Adhesives and Sealants*, McGraw-Hill, New York, 2007.
- [5] M. Charbonnier, M. Romand, Polymer pretreatments for enhanced adhesion of metals deposited by the electroless process, *Int. J. Adhes. Adhes.* 23 (2003) 277–285.
- [6] T.H. Baum, D.C. Miller, T.R. O'Toole, Photoselective catalysis of electroless copper solutions for the formation of adherent copper films onto polyimide, *Chem. Mater.* 3 (1991) 714–720.
- [7] S. Yoon, H.-J. Choi, J.-K. Yang, H.-H. Park, Comparative study between poly(p-phenylenevinylene) (PPV) and PPV/SiO₂ nano-composite for interface with aluminum electrode, *Appl. Surf. Sci.* 237 (2004) 451–456.
- [8] T.-G. Woo, I.-S. Park, K.-W. Seol, Effects of various metal seed layers on the surface morphology and structural composition of the electroplated copper layer, *Met. Mater. Int.* 15 (2009) 293–297.
- [9] T. Duguet, F. Senocq, L. Laffont, C. Vahlas, Metallization of polymer composites by metalorganic chemical vapor deposition of Cu: surface functionalization driven films characteristics, *Surf. Coat. Technol.* 230 (2013) 254–259.
- [10] J. Ge, M.P.K. Turunen, J.K. Kivilahti, Surface modification and characterization of photodefinable epoxy/copper systems, *Thin Solid Films* 440 (2003) 198–207.
- [11] C. Weiss, H. Muenstedt, Surface modification of polyether ether ketone (peek) films for flexible printed circuit boards, *J. Adhes.* 78 (2002) 507–519.
- [12] L. Di, B. Liu, J. Song, D. Shan, D.-A. Yang, Effect of chemical etching on the Cu/Ni metallization of poly (ether ether ketone)/carbon fiber composites, *Appl. Surf. Sci.* 257 (2011) 4272–4277.
- [13] S. Siau, A. Vervaet, E. Schacht, A. Van Calster, Influence of chemical pretreatment of epoxy polymers on the adhesion strength of electrochemically deposited Cu for use in electronic interconnections, *J. Electrochem. Soc.* 151 (2004) C133–C141.
- [14] P.B. Messersmith, J. Dalsin, L. Lin, B.P. Lee, H. K., Polymeric compositions and related method of use, WO 2005/118831 A2, Northwestern University (USA), 2005.
- [15] M. Kemell, E. Färm, M. Ritala, M. Leskelä, Surface modification of thermoplastics by atomic layer deposition of Al₂O₃ and TiO₂ thin films, *Eur. Polym. J.* 44 (2008) 3564–3570.
- [16] G. Cui, D. Wu, Y. Zhao, W. Liu, Z. Wu, Formation of conductive and reflective silver nanolayers on plastic films via ion doping and solid-liquid interfacial reduction at ambient temperature, *Acta Mater.* 61 (2013) 4080–4090.
- [17] X. Gu, T. Nguyen, M. Oudina, D. Martin, B. Kidah, J. Jasmin, A. Rezig, L. Sung, E. Byrd, J. Martin, D. Ho, Y.C. Jean, Microstructure and morphology of amine-cured epoxy coatings before and after outdoor exposures—an AFM study, *J. Coat. Technol. Res.* 2 (2005) 547–556.
- [18] J. Kanzow, P.S. Horn, M. Kirschmann, V. Zaporozhchenko, K. Dolgner, F. Faupel, C. Wehlock, W. Possart, Formation of a metal/epoxy resin interface, *Appl. Surf. Sci.* 239 (2005) 227–236.
- [19] K. Endo, S. Maeda, M. Aida, Simulation of C 1s spectra of C- and O-containing polymers in XPS by ab initio MO calculations using model oligomers, *Polym. J.* 29 (1997) 171–181.
- [20] K. Endo, S. Maeda, Y. Kaneda, Analysis of C 1s spectra of N-, O-, and X-containing polymers in X-ray photoelectron spectroscopy by ab initio molecular orbital calculations using model molecules, *Polym. J.* 29 (1997) 255–260.
- [21] J.C. Slater, K.H. Johnson, Self-consistent-field X_o cluster method for polyatomic molecules and solids, *Phys. Rev. B* 5 (1972) 844–853.
- [22] K. Takaoka, T. Otsuka, K. Naka, A. Niwa, T. Suzuki, C. Bureau, S. Maeda, K. Hyodo, K. Endo, D.P. Chong, Analysis of X-ray photoelectron spectra of electrochemically prepared polyaniline by DFT calculations using model molecules, *J. Mol. Struct.* 608 (2002) 175–182.
- [23] T. Otsuka, K. Endo, M. Suhara, D.P. Chong, Theoretical X-ray photoelectron spectra of polymers by deMon DFT calculations using the model dimers, *J. Mol. Struct.* 522 (2000) 47–60.
- [24] C.E. Miller, Near-infrared spectroscopy of synthetic polymers, *Appl. Spectrosc. Rev.* 26 (1991) 277–339.
- [25] D. Nečas, P. Klapetek, Gwyddion: an open-source software for SPM data analysis, *Centr. Eur. J. Phys.* 10 (2012) 181–188.
- [26] J.H. Scofield, Hartree-Slater subshell photoionization cross-sections at 1254 and 1487 eV, *J. Electron Spectrosc. Relat. Phenom.* 8 (1976) 129–137.
- [27] M.J. Frisch, G.W. Trucks, H.B. Schlegel, G.E. Scuseria, M.A. Robb, J.R. Cheeseman, J.A. Montgomery, J.T. Vreven, K.N. Kudin, J.C. Burant, J.M. Millam, S.S. Iyengar, J. Tomasi, V. Barone, B. Mennucci, M. Cossi, G. Scalmani, N. Rega, G.A. Petersson, H. Nakatsuji, M. Hada, M. Ehara, K. Toyota, R. Fukuda, J. Hasegawa, M. Ishida, T. Nakajima, Y. Honda, O. Kitao, H. Nakai, M. Klene, X. Li, J.E. Knox, H.P. Hratchian, J.B. Cross, C. Adamo, J. Jaramillo, R. Gomperts, R.E. Stratmann, O. Yazyev, J. Austin, R. Cammi, C. Pomelli, J.W. Ochterski, P.Y. Ayala, K. Morokuma, G.A. Voth, P. Salvador, J.J. Dannenberg, V.G. Zakrzewski, S. Dapprich, A.D. Daniels, M.C. Strain, O. Farkas, D.K. Malick, A.D. Rabuck, K. Raghavachari, J.B. Foresman, J.V. Ortiz, Q. Cui, A.G. Baboul, S. Clifford, J. Cioslowski, B.B. Stefanov, G. Liu, A. Liashenko, P. Piskorz, I. Komaromi, R.L. Martin, D.J. Fox, T. Keith, M.A. Al-Laham, C.Y. Peng, A. Nanayakkara, M. Challacombe, P.M.W. Gill, B. Johnson, W. Chen,

- M.W. Wong, C. Gonzalez, J.A. Pople, Gaussian 03, Revision B05, Gaussian, Inc., Pittsburg, PA, 2003.
- [28] L.-A. O'Hare, B. Parbhoo, S.R. Leadley, Development of a methodology for XPS curve-fitting of the Si 2p core level of siloxane materials, *Surf. Interface Anal.* 36 (2004) 1427–1434.
- [29] M. Aufray, A. André Roche, Epoxy–amine/metal interphases: influences from sharp needle-like crystal formation, *Int. J. Adhes. Adhes.* 27 (2007) 387–393.
- [30] P.S. Bagus, E.S. Ilton, C.J. Nelin, The interpretation of XPS spectra: insights into materials properties, *Surf. Sci. Rep.* 68 (2013) 273–304.